Space-time-resolved quantum electrodynamics: A (1+1)-dimensional model

Scott Glasgow and Dallas Smith
Department of Mathematics, Brigham Young University, Provo, Utah 84602, USA

Luke Pritchett, John Gardiner, and Michael J. Ware*
Department of Physics and Astronomy, Brigham Young University, Provo, Utah 84602, USA
(Received 13 April 2016; published 3 June 2016)

We develop a model that reduces quantum electrodynamics (QED) in time plus three spatial dimensions to time plus a single spatial dimension, making it is possible to numerically calculate the dynamic behavior of simple QED systems. The dimensionality is restricted in such a way as to preserve the influence of spin and angular momentum. In contrast to the *S*-matrix scattering approach, these calculations are not perturbative within the zero- and one-photon sector of the relevant Hilbert space. The model restricts the electron occupation number to one and the photon occupation number to zero or one. We use this model to calculate the dynamics of a so-called bare electron that dresses itself by a photon field.

DOI: 10.1103/PhysRevA.93.062106

I. INTRODUCTION

Quantum electrodynamics (QED) provides the most accurate model of one of the most fundamental of physical processes: The interaction between photons and electrons. Particle scattering calculations made using QED agree with beam experiments to a high degree of accuracy. Traditionally, these scattering processes are studied using the perturbative *S*-matrix approach [1], typically depicted using Feymann diagrams. This approach has proven very successful in calculating time-independent quantities such as energies of atomic sublevels and scattering cross sections. However, it provides little insight into the dynamics of intermediate processes that occur between input and output states. For example, bare electrons cannot exist without self-dressing (binding to virtual photons), but producing visualization of the full dynamics of this process is currently intractable with full QED. It is worth exploring how the dynamics of these types of processes unfold.

In the past decade, the group of Grobe, Su, *et al.* have made remarkable strides in qualitatively visualizing time-resolved particle dynamics in these kinds of processes [2–5]. Wagner *et al.* from this group looked at the time evolution of a one-dimensional simplified Hamiltonian based on a Yukawa interaction [4]. These models use a massive boson as an analog to the photon, and neglect spin and polarization. Using this simpler interaction in place of the full Dirac-Maxwell QED Hamiltonian makes numerical simulation in one spatial dimension accessible. They produced animations of a bare fermion being dressed by a boson field as well as scattering processes analogous to Compton scattering.

In this paper, we embark on a similar and complementary agenda to that taken by Grobe, Su *et al.* [2]. In their work, they use simpler models in place of QED and then restrict their second quantized Hamiltonian's action to one spatial dimensional when calculating. These simpler models must make some concessions, such as so-called photons with mass and particles without spin. In our approach, we begin with full QED based on Dirac and Maxwell, but then restrict our analysis to only the simplest of fundamental processes, namely that of a bare electron of a given spin interacting with a massless polarized photon.

Note that our approach is not equivalent to writing down a U(1) gauge theory in 1+1 dimensions, which is known as 1+1 QED or the Schwinger model [6]. The Schwinger model may be solved exactly but has very different phenomenology than 3+1 QED. Instead, we are projecting the Hilbert space of 3+1 QED onto a restricted subspace of states and then solving the projected Hamiltonian. The goal is to create a description that can model phenomenology more analogous to 3+1 QED, such as a bare electron dressing itself with a photon field. We do not expect the projected Hamiltonian to be the Hamiltonian of a local quantum field theory (for example, it does not have antiparticle states). However, we are satisfied as long as it is causal and can reproduce phenomenology analogous to 3+1 QED.

Using our model, we compute the physical fermion or dressed electron of our reduced model. This dressed state is a quantum superposition of bare electron states (without correlated photons) and correlated electron-photon states (in which the bare electron is accompanied by one photon). Using our reduced model and similar to the result in Ref. [4], we find that the mass of the physical fermion is reduced from its bare counterpart by its attachment to a correlated photon. In analogy to the results in Ref. [7], we find that an initially bare, unphysical fermion (electron) rapidly dresses itself with a boson (photon) field to become the physical fermion. The formation of the physical fermion is accompanied by radiation of unneeded photon probability into the ambient space surrounding the dressed fermion.

In contrast with the *S*-matrix scattering approach, these calculations are not perturbative. Our approach can be done in such a way as to preserve the influence of the intrinsic properties of spin and angular momentum and the polarization properties of a massless photon. We calculate the eigenstates of the reduced Hamiltonian for this model in order to construct a dynamical evolution of a bare electron dressing itself.

This article is outlined as follows. In Sec. II, we introduce the well-known full QED Hamiltonian for describing the interactions between charged matter and light fields. In Sec. III,

*ware@byu.edu

we introduce a reduced Hamiltonion that acts in the same way as the full Hamiltonion on a reduced Hilbert space that represents a system with at most one electron and a single photon. We further manipulate the interaction portion of this Hamiltonian into a form that explicitly shows its behavior when electron and photon momenta are restricted to a single dimension. We then construct a reduced Hamiltonian using this interaction term along with reduced versions of the other terms in the Hamiltonian. In Sec. IV we discuss the eigenvalues and eigenvectors of this reduced Hamiltonian. Finally, in Sec. V we illustrate how this reduced Hamiltonian can be used to study the dynamics of a bare electron dressing itself with a photon field.

II. COULOMB GAUGE HAMILTONIAN

Following Cohen-Tannoudji [8], the QED Hamiltonian for the radiation-matter field in the Coulomb gauge can be written as

$$H = H_D + H_R + H_I + V_{\text{Coul}}. \tag{1}$$

The Dirac term H_D acts on the matter field, and is given by

$$H_D = \int d^3\mathbf{r} : \Psi^\dagger(\mathbf{r})\left(\alpha_0 m_0 c^2 + \frac{\hbar c}{i}\boldsymbol{\alpha}\cdot\boldsymbol{\nabla}\right)\Psi(\mathbf{r}) : . \tag{2}$$

The colons indicate that creation and annihilation operators (introduced below) must be normal ordered. The parameter m_0 is the bare mass of an electron and the α_0 and $\boldsymbol{\alpha} = (\alpha_1,\alpha_2,\alpha_3)$ matrices are given by

$$\alpha_0 = \begin{bmatrix} I_{2\times2} & 0_{2\times2} \\ 0_{2\times2} & -I_{2\times2} \end{bmatrix}, \qquad \alpha_j = \begin{bmatrix} 0_{2\times2} & \sigma_j \\ \sigma_j & 0_{2\times2} \end{bmatrix}, \tag{3}$$

with $0_{2\times2}$ representing a 2×2 matrix of zeros, $I_{2\times2}$ representing the 2×2 identity matrix, and σ_j representing the usual Pauli matrices, given by

$$\sigma_1 = \begin{bmatrix} 0 & 1 \\ 1 & 0 \end{bmatrix}, \quad \sigma_2 = \begin{bmatrix} 0 & -i \\ i & 0 \end{bmatrix}, \quad \sigma_3 = \begin{bmatrix} 1 & 0 \\ 0 & -1 \end{bmatrix}. \tag{4}$$

The 4-component matter field Ψ can be written in terms of momentum components as

$$\Psi(\mathbf{r}) = \int d^3\mathbf{p} \frac{e^{i\frac{\mathbf{p}\cdot\mathbf{r}}{\hbar}}}{(2\pi\hbar)^{3/2}} U(\mathbf{p})\boldsymbol{\chi}(\mathbf{p}). \tag{5}$$

The vector $\boldsymbol{\chi}$ is given by

$$\boldsymbol{\chi}(\mathbf{p}) = \begin{bmatrix} c_\uparrow(\mathbf{p}) \\ c_\downarrow(\mathbf{p}) \\ d_\uparrow^\dagger(\mathbf{p}) \\ d_\downarrow^\dagger(\mathbf{p}) \end{bmatrix}, \tag{6}$$

where $c_\uparrow(\mathbf{p})$ and $c_\downarrow(\mathbf{p})$ are the Fermionic annihilation operators for bare spin-up and spin-down electrons with momentum $\mathbf{p}$, and $d_\uparrow^\dagger(\mathbf{p})$ and $d_\downarrow^\dagger(\mathbf{p})$ are the creation operators for bare spin-up and spin-down positrons with momentum $\mathbf{p}$. These operators satisfy the usual Fermionic anticommutation relations

$$\begin{aligned}\{c_\uparrow(\mathbf{p}),c_\uparrow^\dagger(\mathbf{q})\} &= \{c_\downarrow(\mathbf{p}),c_\downarrow^\dagger(\mathbf{q})\} = \{d_\uparrow(\mathbf{p}),d_\uparrow^\dagger(\mathbf{q})\} \\ &= \{d_\downarrow(\mathbf{p}),d_\downarrow^\dagger(\mathbf{q})\} = \delta(\mathbf{p}-\mathbf{q})\mathbf{1},\end{aligned} \tag{7}$$

where $\mathbf{1}$ is the identity operator, with all other anticommutators vanishing. The matrix $U(\mathbf{p})$ is chosen to diagonalize the momentum representation of the operator in parentheses in (2), such that we can write

$$U^\dagger(\mathbf{p})(\alpha_0 p_0 + \mathbf{p}\cdot\boldsymbol{\alpha})U(\mathbf{p}) = \alpha_0\sqrt{p_0^2+p^2}, \tag{8}$$

where $p = \|\mathbf{p}\|$ and $p_0 = m_0 c$. Using $U(\mathbf{p})$, the anticommutators in (7), and normal ordering, we rewrite (2) in the useful form

$$\begin{aligned}H_D = cp_0 \int d^3\mathbf{p}\sqrt{1+\frac{p^2}{p_0^2}}[&c_\uparrow^\dagger(\mathbf{p})c_\uparrow(\mathbf{p}) + c_\downarrow^\dagger(\mathbf{p})c_\downarrow(\mathbf{p}) \\ &+ d_\uparrow^\dagger(\mathbf{p})d_\uparrow(\mathbf{p}) + d_\downarrow^\dagger(\mathbf{p})d_\downarrow(\mathbf{p})].\end{aligned} \tag{9}$$

The radiation term H_R in (1) describes the light field and is given by

$$H_R = \int d^3\mathbf{k}\hbar\omega_{\mathbf{k}}[a_1^\dagger(\mathbf{k})a_1(\mathbf{k}) + a_2^\dagger(\mathbf{k})a_2(\mathbf{k})], \tag{10}$$

where $a_1(\mathbf{k})$ and $a_2(\mathbf{k})$ annihilate photons of wave number $\mathbf{k}$ (with momentum $\hbar\mathbf{k}$ and frequency $\omega_{\mathbf{k}} = c\|\mathbf{k}\|$), while $a_1^\dagger(\mathbf{k})$ and $a_2^\dagger(\mathbf{k})$ create those same photons. The subscripts 1 and 2 refer to two orthogonal polarizations which are also orthogonal to $\mathbf{k}$. These operators satisfy the usual commutation relations, namely

$$[a_1(\mathbf{k}),a_1^\dagger(\mathbf{k}')] = [a_2(\mathbf{k}),a_2^\dagger(\mathbf{k}')] = \delta(\mathbf{k}-\mathbf{k}')\mathbf{1},$$

with all other commutators vanishing. Importantly the bosonic and fermionic operators commute with each other: For example,

$$[a_1(\mathbf{k}),c_\downarrow^\dagger(\mathbf{p})] = 0$$

for all wave numbers $\mathbf{k}$ and momenta $\mathbf{p}$.

The term H_I in (1) describes the interaction of light and matter and is given by

$$H_I = -ec\int d^3\mathbf{r} \; : \Psi^\dagger(\mathbf{r})\boldsymbol{\alpha}\cdot\mathbf{A}_\perp(\mathbf{r})\Psi(\mathbf{r}) : , \tag{11}$$

where e is a free parameter with units of charge, and the transverse, three-component vector potential $\mathbf{A}_\perp$ is the photon field given by

$$\mathbf{A}_\perp(\mathbf{r}) = \int d^3\mathbf{k}\sum_{j=1}^{2}\frac{a_j(\mathbf{k})e^{i\mathbf{k}\cdot\mathbf{r}} + a_j^\dagger(\mathbf{k})e^{-i\mathbf{k}\cdot\mathbf{r}}}{\sqrt{2\epsilon_0\omega_{\mathbf{k}}(2\pi)^3/\hbar}}\boldsymbol{\epsilon}_j(\mathbf{k}). \tag{12}$$

The photon polarizations $\boldsymbol{\epsilon}_1(\mathbf{k})$ and $\boldsymbol{\epsilon}_2(\mathbf{k})$ are transverse to the direction $\mathbf{k}$ of photon propagation and are orthonormal:

$$\boldsymbol{\epsilon}_1(\mathbf{k})\cdot\mathbf{k} = \boldsymbol{\epsilon}_2(\mathbf{k})\cdot\mathbf{k} = \boldsymbol{\epsilon}_1(\mathbf{k})\cdot\boldsymbol{\epsilon}_2(\mathbf{k}) = 0$$

and

$$\boldsymbol{\epsilon}_1(\mathbf{k})\cdot\boldsymbol{\epsilon}_1(\mathbf{k}) = \boldsymbol{\epsilon}_2(\mathbf{k})\cdot\boldsymbol{\epsilon}_2(\mathbf{k}) = 1.$$

The Coulomb term V_{Coul} in (1) describes the self-interaction of the charged matter field and is given by

$$\begin{aligned}V_{\text{Coul}} &= \frac{1}{8\pi\epsilon_0}\iint d^3\mathbf{r}\, d^3\mathbf{r}' \frac{:\rho(\mathbf{r})\rho(\mathbf{r}'):}{\|\mathbf{r}-\mathbf{r}'\|} \\ &= \frac{1}{2\epsilon_0}\int d^3\mathbf{k}\frac{:\hat\rho^\dagger(\mathbf{k})\hat\rho(\mathbf{k}):}{\|\mathbf{k}\|^2},\end{aligned} \tag{13}$$

where the charge density operator ρ in real and reciprocal space is given by

$$\rho(\mathbf{r}) = e\Psi^\dagger(\mathbf{r})\Psi(\mathbf{r}) \tag{14}$$

and

$$\begin{aligned}\hat{\rho}(\mathbf{k}) &= \frac{1}{(2\pi)^{\frac{3}{2}}}\int d^3\mathbf{k} e^{-i\mathbf{k}\cdot\mathbf{r}}\rho(\mathbf{r}) \\ &= \frac{e}{(2\pi)^{\frac{3}{2}}}\int d^3\mathbf{p}\, \boldsymbol{\chi}^\dagger(\mathbf{p})U^\dagger(\mathbf{p})U(\mathbf{p}+\hbar\mathbf{k})\boldsymbol{\chi}(\mathbf{p}+\hbar\mathbf{k}).\end{aligned} \tag{15}$$

III. DERIVATION OF REDUCED HAMILTONIAN

Diagonalizing the full QED Hamiltonian is intractable both computationally and analytically. The interaction term H_I is required to describe nontrivial situations including both matter and light, and V_{Coul} is required to describe interactions between charged particles. But H_I contains 16 individual terms, while V_{Coul} contains an additional 256 terms. This profusion of terms makes it impractical to solve the system, even numerically. In this section, we develop a simplified model for which dynamics can easily be computed using readily available resources by introducing several restrictions and approximations.

Our first simplification is to restrict our model to consider only states with exactly one electron and at most one photon. For this system, the interaction term H_I from (11) can be written in momentum space as

$$H_I = b_I \iint d^3\mathbf{p}' d^3\mathbf{p} \frac{O(\mathbf{p}',\mathbf{p})}{\sqrt{\|\mathbf{p}'-\mathbf{p}\|}} \tag{16}$$

where

$$b_I = -\frac{e}{\hbar^2}\sqrt{\frac{c}{2\epsilon_0(2\pi)^3}} \tag{17}$$

and

$$O(\mathbf{p}',\mathbf{p}) =: \boldsymbol{\chi}^\dagger(\mathbf{p}')B(\mathbf{p}',\mathbf{p})\boldsymbol{\chi}(\mathbf{p}) : \tag{18}$$

with

$$B(\mathbf{p}',\mathbf{p}) = U^\dagger(\mathbf{p}')\boldsymbol{\alpha}\cdot\mathbf{a}_\perp(\mathbf{k})U(\mathbf{p}), \tag{19}$$

where $\mathbf{k} = (\mathbf{p}'-\mathbf{p})/\hbar$ and

$$\begin{aligned}\mathbf{a}_\perp(\mathbf{k}) = {}& a_1(\mathbf{k})\boldsymbol{\epsilon}_1(\mathbf{k}) + a_2(\mathbf{k})\boldsymbol{\epsilon}_2(\mathbf{k}) \\ &+ a_1^\dagger(-\mathbf{k})\boldsymbol{\epsilon}_1(-\mathbf{k}) + a_2^\dagger(-\mathbf{k})\boldsymbol{\epsilon}_2(-\mathbf{k}).\end{aligned} \tag{20}$$

We denote a state with no photons and a single bare spin-up electron of momentum $\mathbf{q}$ as $|\mathbf{q}\rangle = c_\uparrow{}^\dagger(\mathbf{q})|\rangle$, where $|\rangle$ denotes the bare vacuum. Acting on this state with H_I, we have

$$\begin{aligned}H_I|\mathbf{q}\rangle &= H_I c_\uparrow{}^\dagger(\mathbf{q})|\rangle \\ &= b_I \iint d^3\mathbf{p}' d^3\mathbf{p} \frac{O(\mathbf{p}',\mathbf{p})c_\uparrow{}^\dagger(\mathbf{q})|\rangle}{\sqrt{\|\mathbf{p}'-\mathbf{p}\|}}.\end{aligned} \tag{21}$$

Using (6) and (18) we can write the numerator of the integrand in (21) as

$$\begin{aligned}&O(\mathbf{p}',\mathbf{p})c_\uparrow^\dagger(\mathbf{q})|\rangle \\ &=: \begin{bmatrix} c_\uparrow{}^\dagger(\mathbf{p}') \\ c_\downarrow{}^\dagger(\mathbf{p}') \\ \cancel{d_\uparrow(\mathbf{p}')} \\ \cancel{d_\downarrow(\mathbf{p}')}\end{bmatrix}^T B(\mathbf{p}',\mathbf{p}) \begin{bmatrix} c_\uparrow(\mathbf{p}) \\ \cancel{c_\downarrow(\mathbf{p})} \\ d_\uparrow{}^\dagger(\mathbf{p}) \\ d_\downarrow{}^\dagger(\mathbf{p})\end{bmatrix} : c_\uparrow{}^\dagger(\mathbf{q})|\rangle.\end{aligned} \tag{22}$$

The elements that have a slash through them vanish in the computation. The element $c_\downarrow$ annihilates the input state, as do the elements $d_\uparrow$ and $d_\downarrow$ when the indicated normal ordering is applied. After these algebraic simplifications, we restrict our system to a subspace with no electron-positron pairs, so that terms of the form $c_\uparrow^\dagger d_\uparrow^\dagger c_\uparrow^\dagger|\rangle$ are neglected. In this low-energy approximation, we can algebraically manipulate (22) to become

$$\begin{aligned}O(\mathbf{p}',\mathbf{p})c_\uparrow^\dagger(\mathbf{q})|\rangle = \delta(\mathbf{p}-\mathbf{q})[&B_{11}(\mathbf{p}',\mathbf{q})c_\uparrow^\dagger(\mathbf{p}') \\ &+ B_{21}(\mathbf{p}',\mathbf{q})c_\downarrow^\dagger(\mathbf{p}')]|\rangle,\end{aligned} \tag{23}$$

where we have also used the anticommutation rule (7). The subscripts on B_{11} and B_{21} indicate the row and column components of the matrix B.

Our next step is to study how the full interaction Hamiltonian H_I interacts with states with exactly one electron and at most one photon. We will eventually reduce this description to one dimension, so we consider photon wave vectors that are in the $\pm\hat{z}$ directions, with polarizations $\boldsymbol{\epsilon}_1(\pm\hat{z}) = \hat{x}$, and $\boldsymbol{\epsilon}_2(\pm\hat{z}) = \pm\hat{y}$. Under this convention, when an electron of initial momentum $\mathbf{q} = q\hat{z}$ interacts with a photon and ends up with a final momentum $\mathbf{p} = p\hat{z}$, we have

$$B_{11}(\mathbf{p},\mathbf{q}) = 0. \tag{24}$$

It immediately follows that

$$c_\uparrow(\mathbf{p})H_I c_\uparrow{}^\dagger(\mathbf{q})|\rangle = 0. \tag{25}$$

This result indicates that, due to conservation of angular momentum, an electron cannot interact with a photon in one dimension without changing its spin since the photon carries angular momentum. On the other hand, for an electron that does change spin on interacting with a photon, we have

$$\begin{aligned}B_{21}(\mathbf{p},\mathbf{q}) = {}&[s(\mathbf{q}/p_0)c(\mathbf{p}/p_0) - s(\mathbf{p}/p_0)c(\mathbf{q}/p_0)] \\ &\times [a_1^\dagger(\Delta k\hat{\mathbf{z}}) + i\,\text{sign}(\Delta k)a_2^\dagger(\Delta k\hat{\mathbf{z}})]\end{aligned} \tag{26}$$

with $\Delta k = (q-p)/\hbar$ and

$$c(\boldsymbol{\xi}) = \sqrt{\frac{1}{2}\left(1 + \frac{1}{\sqrt{1+\boldsymbol{\xi}\cdot\boldsymbol{\xi}}}\right)}, \tag{27}$$

$$s(\boldsymbol{\xi}) = \eta(\boldsymbol{\xi})\sqrt{\frac{1}{2}\left(1 - \frac{1}{\sqrt{1+\boldsymbol{\xi}\cdot\boldsymbol{\xi}}}\right)}. \tag{28}$$

The function η specifies the sign of the z component of its argument via

$$\eta(\boldsymbol{\xi}) = \boldsymbol{\xi}\cdot\hat{\mathbf{z}}/\|\boldsymbol{\xi}\|. \tag{29}$$

From (26) it immediately follows that

$$c_\downarrow(\mathbf{p})H_I c_\uparrow^\dagger(\mathbf{q})|\,\rangle = b_I \frac{s_q c_p - s_p c_q}{\sqrt{|q-p|}}[a_1^\dagger(\Delta k\hat{\mathbf{z}}) + i\,\mathrm{sign}(\Delta k)a_2^\dagger(\Delta k\hat{\mathbf{z}})]|\,\rangle. \quad (30)$$

where $s_p = s(p\hat{\mathbf{z}})$ and $c_p = c(p\hat{\mathbf{z}})$.

Now we are in a position to introduce a reduced interaction Hamiltonian h_I that acts the same way as the full H_I (16) on the our subset of states. We consider states $|\mathbf{p}\rangle$ that have an electron with momentum $\mathbf{p}$ and no photon, and states $|\mathbf{p},\mathbf{p}'-\mathbf{p}\rangle$ that have an electron with momentum $\mathbf{p}$ and a photon with momentum $\mathbf{p}'-\mathbf{p}$. Using this notation, we can write our reduced interaction Hamiltonian as

$$h_I = \hbar^{\frac{3}{2}} b_I \iint d^3\mathbf{p}'d^3\mathbf{p}\Bigg[\frac{s(\mathbf{p})c(\mathbf{p}') - s(\mathbf{p}')c(\mathbf{p})}{\sqrt{|\mathbf{p}-\mathbf{p}'|}} \times (|\mathbf{p},\mathbf{p}'-\mathbf{p}\rangle\langle\mathbf{p}'| + |\mathbf{p}'\rangle\langle\mathbf{p},\mathbf{p}'-\mathbf{p}|)\Bigg], \quad (31)$$

where

$$|\mathbf{p}\rangle = c_\uparrow^\dagger(\mathbf{p})|\rangle, \quad (32)$$

$$|\mathbf{p},\mathbf{q}\rangle = -\frac{a_1^\dagger(\mathbf{k_q}) + i\eta(\mathbf{q})a_2^\dagger(\mathbf{k_q})}{\sqrt{2\hbar^3}} c_\downarrow^\dagger(\mathbf{p})|\rangle. \quad (33)$$

The wave vector is related to the photon momentum as usual: $\mathbf{k_q} = \mathbf{q}/\hbar$. The definitions (32) and (33) yield the orthonormality conditions

$$\langle\mathbf{q}|\mathbf{p}\rangle = \delta(\mathbf{q}-\mathbf{p}), \quad (34)$$

$$\langle\mathbf{p}',\mathbf{q}'|\mathbf{p},\mathbf{q}\rangle = \delta(\mathbf{q}-\mathbf{q}')\delta(\mathbf{p}-\mathbf{p}'), \quad (35)$$

$$\langle\mathbf{p}'|\mathbf{p},\mathbf{q}\rangle = 0. \quad (36)$$

In preparation for restricting the reduced Hamiltonian (31) to one dimension, we now introduce dimensionless momentum

$$\boldsymbol{\xi} = \mathbf{p}/p_0. \quad (37)$$

In terms of this dimensionless momentum, our basis states can now be written as

$$|\boldsymbol{\xi}\rangle = p_0^{3/2}|\mathbf{p}\rangle, \quad (38)$$

$$|\boldsymbol{\xi},\boldsymbol{\xi}'\rangle = p_0^3|\mathbf{p},\mathbf{p}'\rangle, \quad (39)$$

so that the inner products

$$\langle\boldsymbol{\xi}|\boldsymbol{\xi}'\rangle = \delta(\boldsymbol{\xi}-\boldsymbol{\xi}'), \quad (40)$$

$$\langle\boldsymbol{\xi},\boldsymbol{\xi}'|\boldsymbol{\xi}'',\boldsymbol{\xi}'''\rangle = \delta(\boldsymbol{\xi}-\boldsymbol{\xi}'')\delta(\boldsymbol{\xi}'-\boldsymbol{\xi}''') \quad (41)$$

are unitless. In this basis, the reduced interaction Hamiltonian (31) can be expressed as

$$h_I = cp_0\lambda \iint d^3\boldsymbol{\xi}'d^3\boldsymbol{\xi}\Bigg[\frac{s(\boldsymbol{\xi}')c(\boldsymbol{\xi}) - s(\boldsymbol{\xi})c(\boldsymbol{\xi}')}{\sqrt{|\boldsymbol{\xi}-\boldsymbol{\xi}'|}} \times(|\boldsymbol{\xi},\boldsymbol{\xi}'-\boldsymbol{\xi}\rangle\langle\boldsymbol{\xi}'| + |\boldsymbol{\xi}'\rangle\langle\boldsymbol{\xi},\boldsymbol{\xi}'-\boldsymbol{\xi}|)\Bigg]. \quad (42)$$

The unitless quantity λ is a free parameter given by

$$\lambda = \frac{e}{e_0}\sqrt{\frac{\alpha}{2\pi^2}} \quad (43)$$

which allows one to specify the ratio of e, the charge of the fermion in this reduced model, to the measured charge e_0 of an electron, with α giving the fine structure constant.

We now seek a restricted description that is one dimensional, yet gives qualitatively correct behavior. This will allow for numeric computation with readily available resources. A natural way to project to a single dimension is to reduce the two transverse dimensions in the quantization volume to unit size on the quantization grid. In this situation, the final reduced interaction Hamiltonian becomes

$$\mathcal{H}_I = cp_0\lambda \iint d\xi'd\xi\Bigg[\frac{s_{\xi'}c_\xi - s_\xi c_{\xi'}}{\sqrt{|\xi-\xi'|}} \times(|\xi,\xi'-\xi\rangle\langle\xi'| + |\xi'\rangle\langle\xi,\xi'-\xi|)\Bigg], \quad (44)$$

where $s_\xi = s(\xi\hat{\mathbf{z}})$ and $c_\xi = c(\xi\hat{\mathbf{z}})$. These states have the overlaps

$$\langle\xi\mid\xi'\rangle = \delta(\xi-\xi')$$

and

$$\langle\xi,\xi'|\xi'',\xi'''\rangle = \delta(\xi-\xi'')\delta(\xi'-\xi''')$$

and likewise,

$$\langle\xi|\xi',\xi''\rangle = 0.$$

Using the same techniques that we have used to reduce the interaction Hamiltonian, it is straightforward to show that the reduced Dirac Hamiltonian corresponding to (9) becomes

$$\mathcal{H}_D = cp_0\int d\xi\,\sqrt{1+\xi^2}\left(|\xi\rangle\langle\xi| + \int d\xi'|\xi,\xi'\rangle\langle\xi,\xi'|\right) \quad (45)$$

while the reduce radiation Hamiltonian corresponding to (10) becomes

$$\mathcal{H}_R = cp_0\iint d\xi d\xi'\;\;|\xi'|\;|\xi,\xi'\rangle\langle\xi,\xi'|. \quad (46)$$

The Coulomb potential V_{Coul} in (13) does not contribute to this model. All of the terms resulting from the Coulomb potential involve states with electron-positron pairs in addition to a single electron. We consider only states with exactly one electron in this simplified model, so we exclude these more complex states.

IV. DISCUSSION OF THE REDUCED HAMILTONIAN

We are now ready to write the entire reduced Hamiltonian $\mathcal{H} = \mathcal{H}_D + \mathcal{H}_R + \mathcal{H}_I$ for this model. By combining (44), (45), and (46) and applying some algebraic manipulation to make conservation of total momentum ξ explicit, the final reduced

Hamiltonian becomes

$$\frac{\tilde{\mathcal{H}}}{cp_0} = \int d\xi \Big[E_e(\xi)|\xi\rangle\langle\xi| + \int d\xi' [E_e(\xi') + E_\gamma(\xi-\xi')]|\xi',\xi-\xi'\rangle\langle\xi',\xi-\xi'| + \lambda \int d\xi' g(\xi,\xi')(|\xi',\xi-\xi'\rangle\langle\xi| + |\xi\rangle\langle\xi',\xi-\xi'|)\Big], \tag{47}$$

where

$$g(\xi,\xi') = \frac{s_\xi c'_\xi - s'_\xi c_\xi}{\sqrt{|\xi-\xi'|}} \tag{48}$$

and

$$E_e(\xi) = \sqrt{1+\xi^2}, \tag{49}$$

$$E_\gamma(\xi) = |\xi|. \tag{50}$$

The reduced Hamiltonian is scaled by the rest energy $cp_0 = m_0c^2$ of the bare electron. This energy is a free parameter that sets the energy scale for the model. Since this scaling is arbitrary, it will frequently be convenient to use the unitless reduced Hamiltonian

$$\mathcal{H} = \frac{\tilde{\mathcal{H}}}{p_0 c}. \tag{51}$$

The coupling parameter λ, defined in (43) and used in (48), is also a free parameter which defines the strength of the coupling between the electromagnetic and the charged matter fields. The coupling function g has the property that $g(\xi,\xi')$ approaches zeros as ξ approaches ξ'. Thus, the probability that the electron interacts with a photon but does not change momentum is precisely zero and electrons in this model do not interact with photons of zero momentum.

A. Eigenstates and energies

The eigenstates of the reduced Hamiltonian (47) have the general form

$$|\phi(\xi,E)\rangle = a(\xi,E)|\xi\rangle + \int d\xi' b(\xi',\xi,E)|\xi',\xi-\xi'\rangle. \tag{52}$$

Each eigenstate has a definite total momentum ξ and an energy E, but to enhance readability we suppress these labels below when not needed. The states are comprised of a superposition of a bare electron state $|\xi\rangle$ and an infinite sum of states $|\xi',\xi-\xi'\rangle$. Each state $|\xi',\xi-\xi'\rangle$ has an electron of momentum ξ', a photon of momentum $\xi-\xi'$, and total momentum ξ. The complex coefficients a and $b(\xi')$ specify the relative strength and phase of the components for each eigenstate. The eigenstates fall into two general classes: dressed electron states $|\phi_d\rangle$ with relatively large a coefficients and small $b(\xi')$ coefficients, and correlated electron-photon states $|\phi_{e,\gamma}\rangle$ with small or zero a coefficients and larger contributions from one or more of the $b(\xi')$ coefficients.

Figure 1 plots the energies associated with the two types of eigenstates. The energies of the dressed electron states $|\phi_d\rangle$,

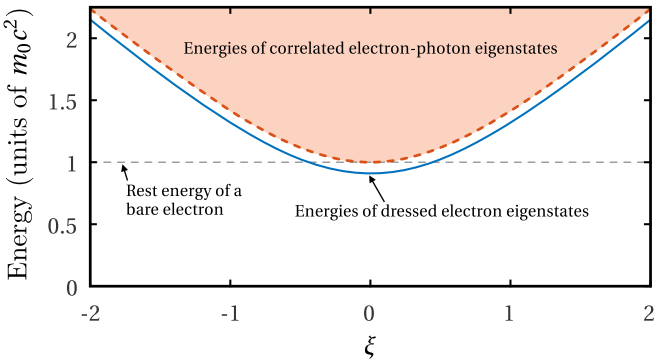

FIG. 1. Energies associated with the eigenstates of the reduced Hamiltonian plotted vs the total momentum ξ of the eigenstate. The solid blue curve shows the energies associated with the dressed electron eigenstates $|\phi_d\rangle$. The shaded red area show the energies for correlated electron-photon states $|\phi_{e,\gamma}\rangle$, with the dashed red line on the bottom showing the energy for states where the photon portion has zero momentum. The horizontal dashed line shows the rest energy of a bare electron.

found by solving the eigenvalue problem

$$\mathcal{H}|\phi_d\rangle = E_d(\xi)|\phi_d\rangle,$$

are plotted as the solid blue line. As expected, the energy of the dressed electron dips below the rest energy of the bare electron, which has a value of one on the plot (in units of m_0c^2). The shaded region in Fig. 1 indicates the possible energies for correlated electron-photon states $|\phi_{e,\gamma}\rangle$. The correlated electron-photon eigenstate with the lowest possible energy for a fixed total momentum ξ is a state of an electron with momentum ξ and a photon with zero momentum, $|\phi_{e,\gamma}\rangle = |\xi,0\rangle$. We find the unitless energy of this type of state to be $E_e(\xi)$:

$$\mathcal{H}|\xi,0\rangle = E_e(\xi)|\xi,0\rangle. \tag{53}$$

The eigenenergies $E_e(\xi) = \sqrt{1+\xi^2}$ are plotted as the dashed red curve in Fig. 1. Note that this result is independent of the coupling parameter λ. Equation (53) holds precisely because $g(\xi,\xi) = 0$, as noted above.

There are also eigenstates independent of λ that take the form

$$|\phi_{e,\gamma}\rangle \propto g(\xi,\xi'_e)|\xi_e,\xi-\xi_e\rangle - g(\xi,\xi_e)|\xi'_e,\xi-\xi'_e\rangle, \tag{54}$$

provided the two components have different electron momenta $\xi_e \neq \xi'_e$, but the same bare energy $E_e(\xi_e) + E_\gamma(\xi-\xi_e) = E_e(\xi'_e) + E_\gamma(\xi-\xi'_e)$. For these states, the dressed energy eigenvalue is the common value $E(\xi,\xi_e) = E_e(\xi_e) + E_\gamma(\xi-\xi_e)$, i.e., the dressed and bare energies are the same, again independent of the coupling parameter λ. There is another set of correlated electron-photon eigenvectors of the form

$$|\phi'_{e,\gamma}\rangle \propto g(\xi,\xi_e)\,|\xi_e,\xi-\xi_e\rangle + g(\xi,\xi'_e)\,|\xi'_e,\xi-\xi'_e\rangle + O(\lambda^2). \tag{55}$$

These states, together with the eigenvectors in (54) and the dressed electron states $|\phi_d\rangle$, form a complete orthonormal set.

Figure 2 plots the energy eigenvalues for the correlated electron-photon eigenstates with $\lambda = 0.4$ vs the total

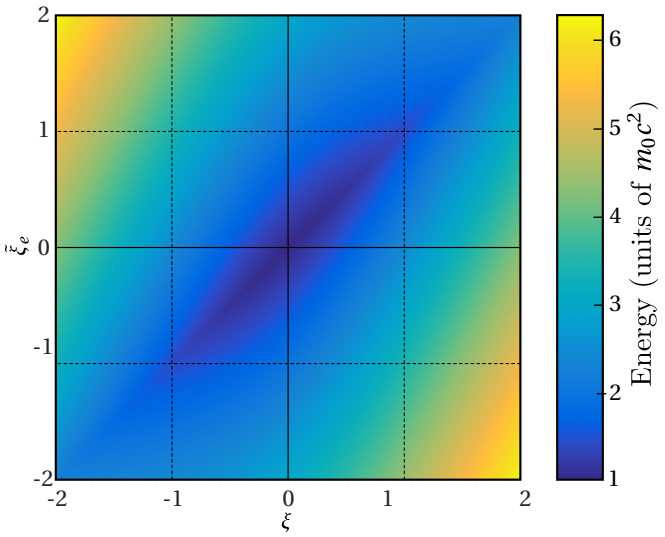

FIG. 2. Energies of the correlated electron-photon eigenstates $|\phi_{e,\gamma}\rangle$ plotted vs the total momentum ξ and the most probable electron momentum $\tilde{\xi}_e$. These eigenstates do not strictly have a single electron momentum, but typically one of the electron momenta is much more probable than all of the others.

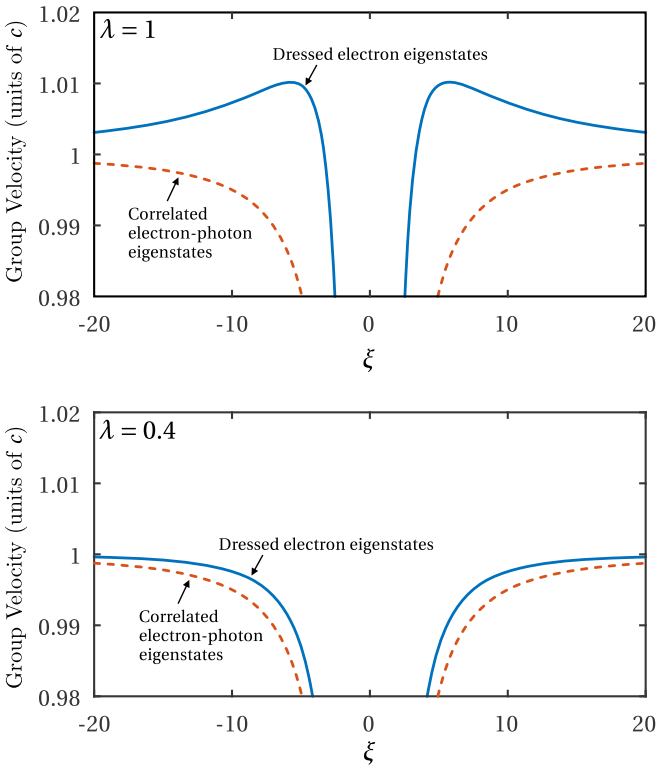

FIG. 3. Absolute value of the group velocity for the dressed electron states (solid blue) and the correlated electron-photon states (dashed red) plotted vs the total momentum ξ of the state. The top plot is for a coupling parameter value of $\lambda = 1$, and the dressed electron states have a group velocity exceeding the speed of light (one) so that the system is acausal. The bottom plot is for a coupling of $\lambda = 0.4$, and group velocities for both types of states remain causal and approach the speed of light for large values of total momentum.

momentum ξ and the most probable electron momentum $\tilde{\xi}_e$. As one would expect, the lowest energy state occurs at zero total momentum with larger energies for larger momenta. These states do not have a well-defined electron momentum since, for example, states of the form (54) explicitly include electron momenta ξ_e and ξ_e'. However, typically one of the electron momenta is much more probable than the other, and that most probable momentum is used on the $\tilde{\xi}_e$ axis to plot the energy distribution.

In Fig. 2, the energy eigenvalues for both types of correlated electron-photon eigenstates, given in (54) and (55), smoothly interleave in the numerical computation. Since half of those eigenvalues are given by the bare energy $E(\xi,\tilde{\xi}_e)$, the other half must also be given by this function. The fact that the energy spectrum of the eigenvectors in (55) does not depend on λ may initially be surprising, but agrees with a result established by Van Hove regarding energy corrections of systems with continuous spectra [9]. We also numerically verified this result by comparing the energies plotted in Fig. 2, found by looking for the most probable ξ_e, with a direct plot of the function $E(\xi,\xi_e)$ and found that they approach the same values as the number of points in the calculation is increased. This indicates that all energy eigenvalues for the correlated electron-photon states are independent of λ, even while half of the eigenvectors do depend on λ. The lower boundary of the energy plot in Fig. 2 matches the dashed red curve in Fig. 1 when the $\tilde{\xi}_e$ dimension is compressed. The shaded region in Fig. 1 shows the other possible energies for different values of $\tilde{\xi}_e$ at the same ξ.

B. Choosing the coupling parameter λ

While the full QED Hamiltonian (1) corresponds to a local field theory, the process that we have used to derive the reduced Hamiltonian does not guarantee that the reduced model is also local and causal. The group velocity v_g for dressed electron states is given by the derivative $v_g(\xi) = dE_d(\xi)/d\xi$. To retain causality, the free parameter λ must be chosen such that the magnitude of $v_g(\xi)$ is always less than the speed of light (i.e., less than one in our scaled units) for all values of ξ. In Fig. 3, we have plotted $|v_g(\xi)|$ for the dressed electron states $|\phi_d\rangle$ with $\lambda = 1$ (top) and $\lambda = 0.4$ (bottom) as the solid blue line. Notice that with $\lambda = 1$, the group velocity exceeds the speed of light for a range of ξ values before returning to causality. This behavior shows that the dressed electron energies for $\lambda = 1$ (analogous to the energies plotted as the blue line in Fig. 1 for $\lambda = 0.4$) do not take the form $E(\xi) = \sqrt{m_p^2 + \xi^2} + E_0$, where m_p is a unitless renormalized physical mass and E_0 is an arbitrary energy offset. Thus, this model is not fully relativistically invariant for all values of λ. However, for $\lambda = 0.4$ the velocities remain less than one everywhere in the range of interest, so the model remains causal in this frame and for this coupling strength. At large values of ξ, the velocities approach the speed of light exactly, independent of λ.

The dashed red curves in both panels in Fig. 3 show the group velocity for the lowest energy correlated electron-photon states (corresponding to the dashed red line in Fig. 1). These group velocities remain below the speed of light for both values of λ. In fact, causality is retained for these states with all values

of λ because, as discussed above, the energies of these states are independent of the choice of λ.

C. Choosing a discretization grid

When choosing a discretization grid for computational purposes, one selects a number N of discrete total momenta to consider and a maximum total momentum $\xi_{\max}$, and then replaces the integrals in (47) with finite sums. These choices determine the range of momenta that are represented in the system and also the energies of the momentum eigenstates. Ideally, these will be chosen such that the coarseness of the grid together with the momentum cutoff do not overly influence the result while optimizing numerical efficiency. Even when modeling dynamics for an electron at rest, the higher momentum states are needed to represent the dressed electron. Typically, one would determine the maximum practical N possible for a given modeling system, and then adjust $\xi_{\max}$ to minimize the errors introduced in discretization.

To measure the errors introduced by discretization, we study the energy eigenvalue for the zero-momentum dressed electron state $|\phi_d(\xi = 0)\rangle$. This state has the minimum energy eigenvalue, and hence represents the rest mass for the dressed electron in this model. This energy eigenvalue can be found exactly by solving the eigenvalue problem $\mathcal{H}|\phi_d(\xi = 0)\rangle = E_{\min}|\phi_d(\xi = 0)\rangle$. After some algebra, this results in

$$E_{\min} = 1 - \lambda^2 \int d\xi' \frac{[g(\xi',0)]^2}{\sqrt{1+\xi'^2} + |\xi'| - E_{\min}},$$

where the integral can be computed analytically to find a transcendental equation for $E_{\min}$. When computing with a finite N and $\xi_{\max}$, the lowest numerical energy eigenvalue will be somewhat higher than $E_{\min}$ due to the discrete nature of the grid. We denote this numerical lowest energy as $\tilde{E}_{\min}$, and study the behavior of $\tilde{E}_{\min}$ as N and $\xi_{\max}$ are varied. In regions where the grid has adequate width and resolution, the value of $\tilde{E}_{\min}$ will near $E_{\min}$ and will not be sensitive to changes of N and $\xi_{\max}$.

Figure 4 plots $\tilde{E}_{\min}$ as N is varied for several values of $\xi_{\max}$. This plot is made for a coupling of $\lambda = 0.4$. The dashed horizontal line near the bottom of the plot shows $E_{\min}$, and the curves show the approximate value $\tilde{E}_{\min}$ obtained for a finite value for N and $\xi_{\max}$. For a given $\xi_{\max}$, the curve flattens out as N is increased, showing the minimum value of N needed to represent a grid with that $\xi_{\max}$. As $\xi_{\max}$ increases, additional points are required to reach this stable region in the energy eigenvalues, and the stable region more closely approaches the exact value $E_{\min}$.

One can also choose a grid by determining the maximum N available for practical computations on a given computer system and then choose $\xi_{\max}$ to minimize the error in the energy eigenvalues. Figure 5 plots $\tilde{E}_{\min}$ as $\xi_{\max}$ is varied for a fixed N. As expected, when a larger N is available for computation, one can more accurately represent a system with a higher $\xi_{\max}$. The plot also shows that there is a preferred $\xi_{\max}$ which minimizes the error for a given value of N.

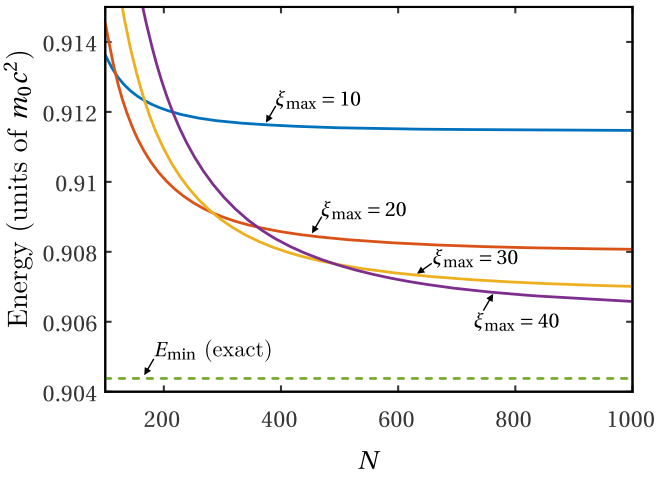

FIG. 4. Value of the minimum energy eigenvalue $\tilde{E}_{\min}$ as the number of points N is varied with a fixed maximum momentum $\xi_{\max}$, compared to the exact rest energy $E_{\min}$ of the dressed electron. Once a minimum N is reached, the accuracy tends to flatten out with additional points (note the compressed energy scale on the left).

V. A BARE ELECTRON DRESSING ITSELF

As an example of the use of this reduced model, we now compute the dynamics of an initially bare electron dressing itself with photon states. For this computation, we choose $N = 256$ and $\xi_{\max} = 23$, as suggested by Fig. 5. We calculate the dynamics of this system using the usual abstract Schrödinger equation

$$i\hbar\frac{\partial}{\partial t}|\Psi(t)\rangle = \tilde{\mathcal{H}}|\Psi(t)\rangle \tag{56}$$

with solution

$$|\Psi(t)\rangle = \exp\{-it\tilde{\mathcal{H}}/\hbar\}|\Psi(t=0)\rangle = \exp\{-i\tau\mathcal{H}\}|\Psi(\tau=0)\rangle, \tag{57}$$

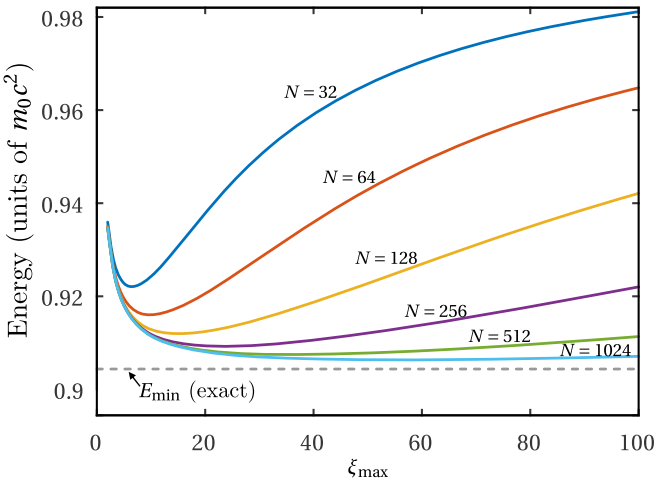

FIG. 5. Value of the minimum energy eigenvalue $\tilde{E}_{\min}$ as $\xi_{\max}$ is varied with a fixed N, compared to the exact rest energy $E_{\min}$ of the dressed electron. Note that each $\tilde{E}_{\min}$ curve has a minimum error at a specific value of $\xi_{\max}$.

where we have introduced the scaled, unitless time $\tau = (p_0 c/\hbar)t$. In the following we use this scaled time and write $|\Psi(\tau)\rangle$ as shorthand for $|\Psi(\tau\hbar/p_0 c)\rangle = |\Psi(t)\rangle$.

We divide the spatial wave function representing this state into two portions:

$$|\Psi(\tau)\rangle = \int dx \Psi_e(x,\tau)|x\rangle + \iint dx dy \Psi_{e,\gamma}(x,y,\tau)|x,y\rangle, \tag{58}$$

where

$$|x\rangle = \int d\xi \frac{e^{-i\xi x}}{\sqrt{2\pi}}|\xi\rangle$$

and

$$|x,y\rangle = \int d\xi' \int d\xi \frac{e^{-i(\xi' x+\xi y)}}{2\pi}|\xi',\xi\rangle.$$

The spatial coordinate x is a scaled unitless quantity related via $x = p_0\tilde{x}/\hbar$ to the spatial coordinate $\tilde{x}$ with units, and similarly for y. The overlap

$$\Psi_{e,\gamma}(x,y,\tau) = \langle x,y|\Psi(\tau)\rangle$$

gives the probability amplitude of finding a bare electron at position x and a photon at position y at time τ. The probability density of finding a bare electron at x that is correlated with a photon at any position then becomes

$$P_{e,*}(x,\tau) = \int dy |\Psi_{e,\gamma}(x,y,\tau)|^2.$$

Likewise, the probability density of finding a photon at a position y, is given by

$$P_{*,\gamma}(y,\tau) = \int dx |\Psi_{e,\gamma}(x,y,\tau)|^2.$$

Finally, the probability density of finding a bare electron at position x with no correlated photon is given by

$$P_e(x,\tau) = |\Psi_e(x,\tau)|^2,$$

where

$$\Psi_e(x,\tau) = \langle x|\,\Psi(\tau)\rangle.$$

To create a localized initial spatial distribution, we begin the system with an initial state defined in momentum space by a Gaussian distribution of bare electron states

$$|\Psi(\tau=0)\rangle = \frac{1}{\sqrt{w\sqrt{\pi/2}}}\int d\xi e^{-\xi^2/w^2}|\xi\rangle. \tag{59}$$

Of course, to compute the evolution, the initial state is represented in terms of the energy-momentum eigenstates using

$$|\Psi(\tau=0)\rangle = \sum_{\xi,E} c_E(\xi)|\phi_E(\xi)\rangle, \tag{60}$$

where $c_E(\xi) = \langle\phi_E(\xi)|\Psi(\tau=0)\rangle$. Then $\mathcal{H}$ in (57) may be replaced by E for each term in (60) to yield

$$|\Psi(\tau)\rangle = \sum_{\xi,E} c_E(\xi)\exp(-i\tau E)|\phi_E(\xi)\rangle. \tag{61}$$

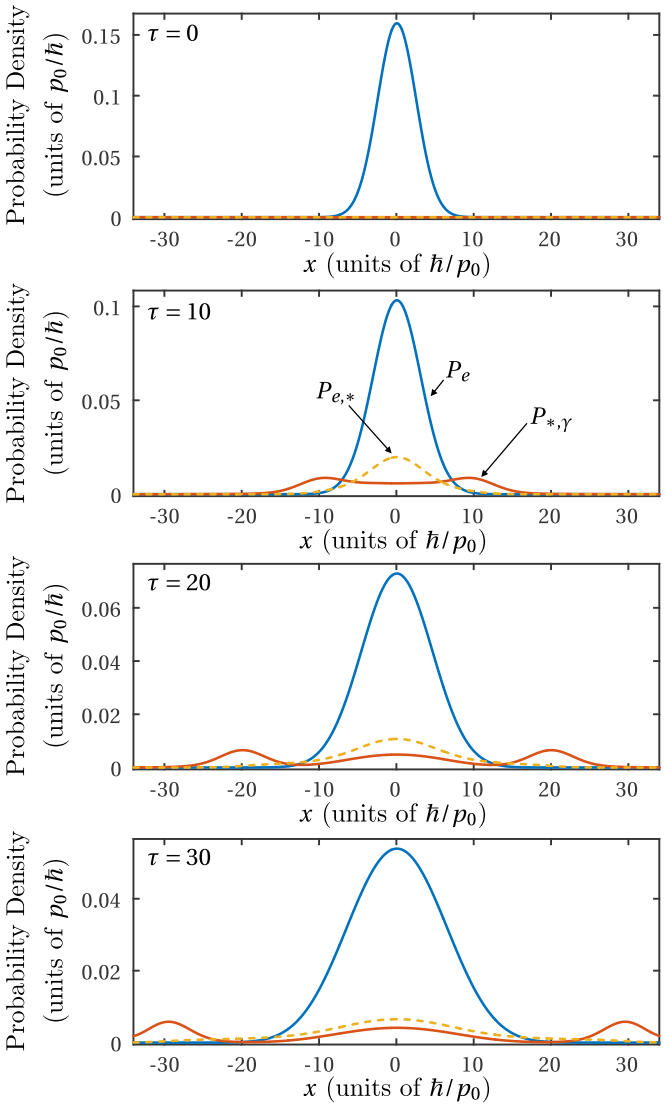

FIG. 6. Animation of a bare electron in an initial superposition of bare electron states $|\xi\rangle$ with a Gaussian distribution in momentum also makes a Gaussian spatial distribution. The probability amplitude of measuring a bare electron state at x is $P_e(x)$, the probability amplitude of measuring a correlated electron-photon state with the electron at x and the photon anywhere is $P_{e,*}(x)$, and the probability of measuring a photon at x and the electron anywhere is $P_{*,\gamma}(x)$.

Figure 6 plots $P_{e,*}$, $P_{*,\gamma}$, and P_e as a function of their spatial coordinate at a sequence of times τ. The distribution width is $w = 0.4$. At $\tau = 0$ the probability of measuring a state with a photon is zero, consistent with (59). As time progresses, the bare electron proceeds to dress itself with a photon field that remains localized around the electron. Meanwhile, there is an additional portion of the photon field that is radiated from the electron and travels precisely at the speed of light. x

We can also place the system directly in the dressed electron state by setting the initial conditions such that

$$|\Psi(\tau=0)\rangle = \frac{1}{\sqrt{w\sqrt{\pi/2}}}\int d\xi e^{-\xi^2/w^2}|\phi_d(\xi)\rangle, \tag{62}$$

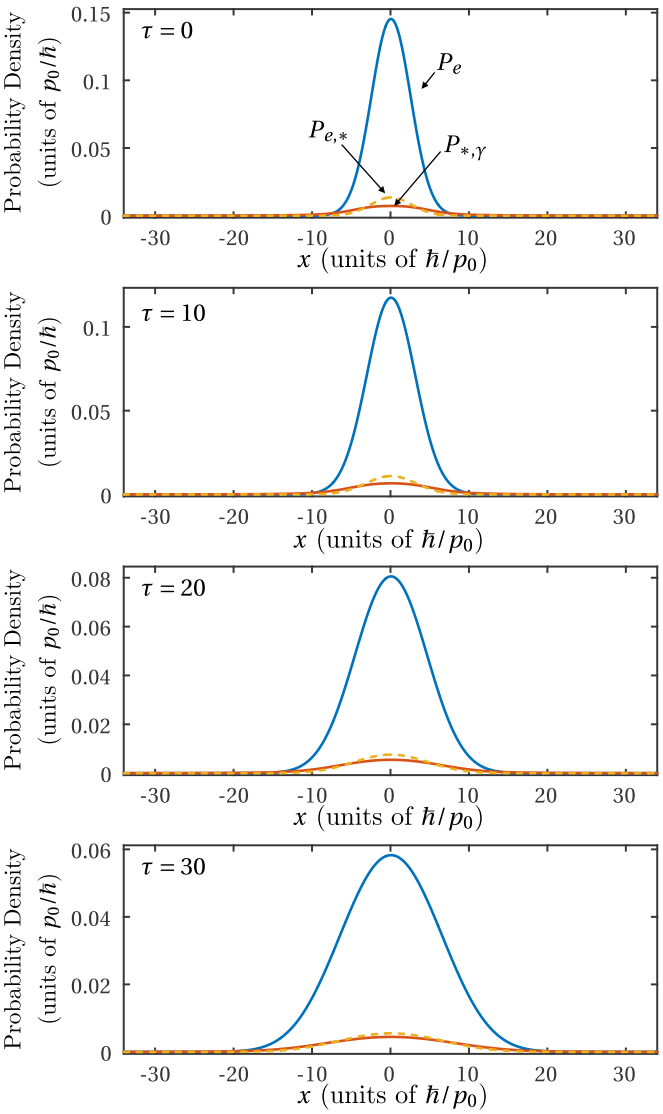

FIG. 7. Animation of a dressed electron in an initial superposition of dressed electron states $|\phi_d\rangle$ with a Gaussian distribution in momentum also makes a Gaussian spatial distribution. The probability amplitude of measuring a bare electron state at x is $P_e(x)$, the probability amplitude of measuring a correlated electron-photon state with the electron at x and the photon anywhere is $P_{e,*}(x)$, and the probability of measuring a photon at x and the electron anywhere is $P_{*,\gamma}(x)$. Note that all distributions exhibit only simple quantum spreading as time τ increases, with fixed distributions in momentum space.

where the eigenstates $|\phi_d\rangle$ correspond to the dressed electron eigenstates discussed in connection with Fig. 1. The system propagates forward in time according to

$$|\Psi(\tau)\rangle = e^{-i\mathcal{H}\tau}|\Psi(\tau=0)\rangle = \frac{1}{\sqrt{w\sqrt{\pi/2}}}\int d\xi e^{-\xi^2/w^2} e^{-iE_d(\xi)\tau}|\phi_d(\xi)\rangle. \quad (63)$$

Figure 7 plots the evolution of this initial state as time proceeds. In this case the electron begins in the physical state with its surrounding photon field and simply spreads due to the usual quantum dispersion. In this case, there are no radiated photons emitted from the electron.

VI. CONCLUSION

We have introduced a reduced QED model for describing an electron field with occupation one interacting with a photon field of occupation zero or one. This model provides a self-consistent method for studying the fundamental interactions between electrons and light as long as the energies are sufficiently low that pair production and multiphoton states can be neglected. In contrast to prior QED methods that rely on scattering theory, this model allows us to study the dynamics of systems with a single electron and a single photon as the interaction occurs. This model describes dynamics in time plus a single spatial dimension in a manner that is consistent with fully three-dimensional QED. We have used this model to visualize the process of a bare electron dressing itself by a photon field. Given the relatively light computing power required for this one-dimensional simulation, we are hopeful that in the near future this work can be extended to two and possibly three spatial dimensions. This work represents a foundational first step toward this goal. Alternatively, one might increase the available photon occupation numbers while remaining in one dimension. We also hope to extend this work to visualize the dynamics of Compton scattering. The ability to study these dynamics can create increased intuition about how these fundamental systems behave.

ACKNOWLEDGMENTS

This work was supported by the National Science Foundation (Grant No. PHY-0970065). We thank Justin Peatross for helpful conversations and editing the manuscript.

[1] M. E. Peskin and D. V. Schroeder, *An Introduction to Quantum Field Theory* (Westview Press, Boulder, CO, 1995).
[2] T. Cheng, E. R. Gospodarczyk, Q. Su, and R. Grobe, Numerical studies of a model fermionboson system, Ann. Phys. (N.Y.) **325**, 265 (2010).
[3] R. E. Wagner, Q. Su, and R. Grobe, Time-resolved Compton scattering for a model fermion-boson system, Phys. Rev. A **82**, 022719 (2010).
[4] R. E. Wagner, M. R. Ware, Q. Su, and R. Grobe, Space-time properties of a boson-dressed fermion for the Yukawa model, Phys. Rev. A **82**, 032108 (2010).
[5] R. E. Wagner, M. R. Ware, B. T. Shields, Q. Su, and R. Grobe, Space-Time Resolved Approach for Interacting Quantum Field Theories, Phys. Rev. Lett. **106**, 023601 (2011).
[6] J. Schwinger, The theory of quantized fields, I, Phys. Rev. **82**, 914 (1951).

[7] T. Cheng, C. C. Gerry, Q. Su, and R. Grobe, Transfer of source correlations to counter-propagating bosons, Europhys. Lett. **88**, 54001 (2009).

[8] C. Cohen-Tannoudji, J. Dupont-Roc, and G. Grynberg, *Photons and Atoms: Introduction to Quantum Electrodynamics* (Wiley, New York, 1997).

[9] L. Van Hove, Energy corrections and persistent perturbation effects in continuous spectra, II: The perturbed stationary states, Physica **22**, 343 (1956).